Int. J. Electrochem. Sci., 14 **(2019)** 3628 – 3643, doi: 10.20964/2019.04.51

International Journal of
ELECTROCHEMICAL
SCIENCE
www.electrochemsci.org

Influence of Pore Aperture and Pore Density on Photoelectrochemical Performance of Titanium Dioxide Nano-Porous Thin Films

Li Fei-hui, Gong Yun-lan[*], *Gao Jing-han*

Department of Applied Chemistry, College of Biotechnology and Food Science, Tianjin University of Commerce, Tianjin, China, 300134
[*]E-mail: tjcugyl@126.com

Received: 14 September 2018 / *Accepted:* 13 February 2019 / *Published:* 10 March 2019

In this paper, preparation of titanium dioxide nano-porous thin films was conducted by electrochemical anodic oxidation. Fluorescence spectrometry, UV-vis absorption spectrometry and electrochemical methods, including electrochemical impedance spectroscopy, chronoamperometry and open-circuit potential time curve test, were used to characterize the photoelectrochemical performance of titanium dioxide nano-porous thin films. Effects of the pore structure, such as average aperture and pore density, on the photoelectrochemical performance of titanium dioxide nano-porous thin films were investigated in detail. The results revealed that TiO_2 nano-porous thin films showed much better photoelectrochemical properties under the illumination of simulated sunlight. The larger the specific surface area, the better the photoelectrochemical performance. When the average aperture and pore density were 103 nm and 1×10^9 cm^{-2}, TiO_2 nano-porous thin film exhibited the optimum photoelectrochemical performance.

Keywords: TiO_2; nano-porous; average aperture; pore density; anodic oxidation

1. INTRODUCTION

Nowadays, titanium dioxide has been widely researched for its abundant resource, low price and pollution-free to environment [1-5]. Owing to its good self-stability, high photocatalytic activity and nontoxic to humans, TiO_2 has been considered to be the best photocatalyst and shows a great potential research and application value in the fields of optics, microelectronics, chemical, energy, biology, medicine, environment and so on [6]. However, since its band gap is wide, TiO_2 only responds to ultraviolet radiation (UV) in sunlight, which reduces its utilization of solar energy and

restricts its application in solar cells. Because the spectral response range of TiO_2 could extend from the UV range into the visible region through dye-sensitization or dimensions reduction to nanometer magnitude [7–9], research on the preparation and performance improvement of TiO_2 nano-materials and dye-sensitized TiO_2 materials have attracted more and more attention.

Although research works on the dimension-reduction of TiO_2, for instance, preparation of TiO_2 nanopowder, TiO_2 nanotubes, TiO_2 nano-porous thin films and so on, have been widely reported [10-14], only a few literatures relate to the discussion and analysis of the relationship between nano stucture and performance of TiO_2 nano-materials. In addition, only a few researchers use electrochemical techniques to complete the preparation and characterization of TiO_2 nano-materials. In fact, there is a strong correlation between the structure and properties of TiO_2 nano-materials. In addition, electrochemical technique possesses many advantages, such as simple, versatile, easy operation, low cost, mild condition and structure of TiO_2 nano-materials can be easily controlled through adjusting electrochemical anodic oxidation parameters, so it would be a good choice to prepare and characterize TiO_2 nano-materials using electrochemical method.

In the present work, our research was focus on the exploration of relationship between pore stucture and performance. TiO_2 nano-porous thin films with different average aperture and pore density were firstly prepared by electrochemical anodic oxidation. Then the influences of average aperture and pore density on the photoelectrochemical properties and the specific surface area of the TiO_2 nano-porous thin films were studied by fluorescence spectrometry, UV-vis absorption spectrometry and electrochemical method. The results are presented here.

2. EXPERIMENTAL

2.1 Chemicals and materials

Redistilled water was used in the preparation of various solutions to ensure the stability of ions in them and all the chemicals used in the experiment were of analytical grade.

2.2 Pretreatment of metal titanium

Thickness and purity of the titanium foil (TA2, Shenzhen Hua Guan Industrial Equipment Co., Ltd.) used in our research was 0.15 mm and 99.5%. Pretreatment of titanium foil was conducted before anodic oxidation to realize the removal of natural oxide film, grease and dust on it and ensure the cleanliness of the surface [15]. The pretreatment steps are as follows: Firstly, the titanium foil was cut into small pieces with a width of 20 mm and a length of 80 mm. Then non-reaction region and non-conductive part of the titanium foil were covered with slide glasses and resin, and the area of the reaction region reserved was 15 mm × 15 mm. Afterward, the reaction region of titanium foil was wiped by acetone defatted cotton, soaked in NaOH solution (5%, 50℃) and H_2SO_4 solution (0.5%, 25℃) for 5 min and 10 s, successively. Rinsing of the reaction region with deionized water was needed between each step mentioned above. Then to further remove the grease from the reaction

region surface, cathodic electrochemical degreasing of titanium foil was performed in an alkaline solution using platinum sheet as a counter electrode. Finally, the reaction region was rinsed with redistilled water again and all the pretreatment process was completed.

2.3 Preparation of TiO_2 nano-porous films

After pretreatment, the reaction region of titanium foil was electrochemical anodic oxidized in H_2SO_4 solution (0.5 mol·l^{-1}) using a two-step voltage mode to prepare TiO_2 nano-porous films. Detailed preparation method was reported in our earlier published research papers [16]. Two steps applied with different voltage were involved in this preparation process, and we defined these two voltages as 'initial voltage' and 'discharge voltage'.

2.4 Characterization of TiO_2 nano-porous films

Morphology of titanium oxide thin films was characterized by JEOL JSM-6700F scanning electron microscope (SEM). Five micro-holes were randomly selected and measured on the SEM image and the average values of the above apertures (i.e. average aperture $\bar{d}$) were calculated. Count the number of holes in the area of a unit scale on the SEM image and number of holes per square centimeter (i.e. pore density ρ) can be calculated. Taking Figure 1 as an example, the calculation method of average aperture and pore density was illustrated as follows.

Calculation method of average aperture: as shown in Figure 1, five micro-holes were selected from the SEM image and their average aperture values could be calculated according to formula 1:

$$\bar{d} = (169\ \text{nm} + 163\ \text{nm} + 209\ \text{nm} + 200\ \text{nm} + 204\ \text{nm})/5 = 189\ \text{nm} \quad (1)$$

Calculation method of pore density: as shown in Figure 1, a scale area (S) equals to 4 μm^2 was selected according to the ruler, while number of microholes (n) in the scale area was 28, so the pore density could be calculated on the basis of formula 2:

$$\rho = S/n = 28/(4\ \mu\text{m}^2) = 7\times10^8\ \text{cm}^{-2} \quad (2)$$

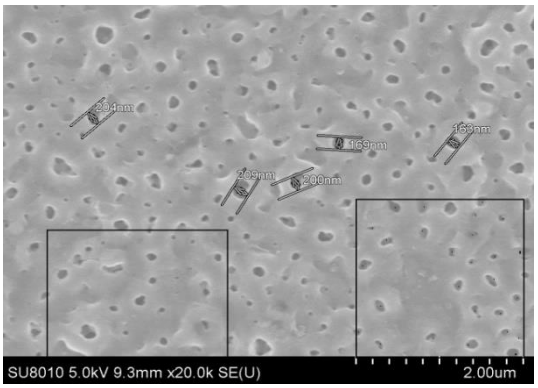

Figure 1. SEM image of TiO_2 nano-porous film

Various electrochemical testing methods, such as electrochemical impedance spectroscopy (EIS), chronoamperometry and open circuit potential (E_{ocp}) time curve test, were used to characterize

the photoelectrochemical properties of TiO_2 nano-porous films. All the electrochemical tests were carried out at room temperature by CHI660E electrochemical working station (Beijing Chinese Science days Techology Co., Ltd.). And the testing process were completed using a standard three-electrode system, which consisted of a platinum plate as the auxiliary electrode, the TiO_2 nano-porous film as the working electrode, a saturated calomel electrode (SCE) as the reference electrode and Na_2SO_4 solution (0.25 $mol \cdot l^{-1}$) as the electrolyte (as shown in figure 2).

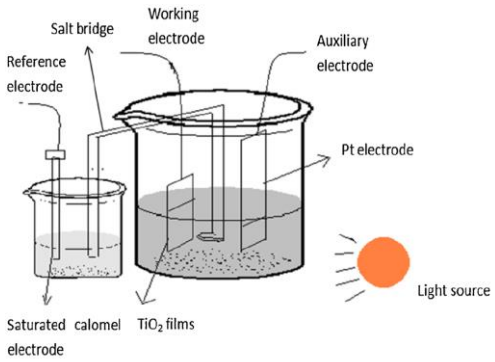

Figure 2. Schematic view of the three-electrode system

During the testing process, the three-electrode system was placed in a photochemical reaction device (Beijing NBET Technology Co., Ltd.), which is equipped with a built-in Solar-500 Xenon lamp source to simulate sunlight. The position of the three-electrode system was adjusted by adjusting the height of the elevator in the device to ensure that the simulating sunlight could be vertically irradiated on the surface of the TiO_2 nano-porous film.

Electrochemical impedance spectra were tested under E_{ocp} in the frequency range of 10 mHz ~ 100 kHz and the applied potentials amplitude was 5 mV. The obtained EIS were simulated by software ZSimpWin using the following equivalent circuit diagram (shown in figure 3).

Figure 3. Equivalent circuit diagram used to simulate the electrochemical impedance spectra

In the testing process of open-circuit potential time (E_{ocp}~t) curves, light irradiation and non-light irradiation was alternately applied to the samples with the alternating period and total testing time of 100 s and 400 s, respectively.

Chronoamperometric curves were recorded under the condition of non-light irradiation. The initial potential, high limit of potential scan, potential difference, initial step direction and potential pulse width were set as E_{ocp}, E_{ocp}, 10 mV, negative and 25 ms, respectively. And the specific surface area was calculated via the following equation.

$$Q = \int_0^t idt \qquad (3)$$

$$C_d = \frac{dq}{d\varphi} = \frac{Q}{\Delta\varphi} = \frac{\int_0^t idt}{\Delta\varphi} \quad (4)$$

$$S_{real} = \frac{C_d}{C_N}, \quad C_N = 20\mu F / cm^2 \quad (5)$$

$$S_{specific} = \frac{S_{real}}{S_{apparent}} \quad (6)$$

where Q is the charge quantity of electric double layer, i is the response current, $\Delta\varphi$ is the potential difference, C_d is the charging capacitor of electric double layer, C_N is the standard capacitor of mercury electrode, S_{real} is the real surface area, $S_{apparent}$ is the apparent surface area and $S_{specific}$ is the specific surface area.

Fluorescence spectra and UV-vis absorption spectra of the TiO_2 nano-porous films were characterized by fluorescence spectrophotometer (Jobin Yvon FL3-212-Tcspc) and UV-visible spectrometer (Hitachi UV-4100) in the wavelength range of 300 ~700 nm and 200~800 nm, separately. The excitation wavelength of fluorescence spectra is 370 nm.

3. RESULTS AND DISCUSSION

3.1 Effects of pore density on the photoelectrochemical properties of TiO_2 nano-porous thin films

In order to investigate the effects of pore density on the photoelectrochemical performance of TiO_2 nano-porous thin films, a group of samples with different pore density but average apertures of about 105 nm were prepared according to our earlier research [15, 19]. The details of the preparation parameters and the average aperture and pore density of the samples are given in Table 1.

Table 1. Preparation parameters of TiO_2 nano-porous films with ρ of 0.4×10^9 cm^{-2} (a) ρ of 0.8×10^9 cm^{-2} (b) ρ of 1.0×10^9 cm^{-2} (c) and ρ of 1.2×10^9 cm^{-2} (d).

Sample	$\bar{d}$ (nm)	ρ ($\times10^9$ cm^{-2})	Initial voltage-discharge voltage (V)	Electrolyte concentration ($mol\cdot l^{-1}$)	Time (min)	Temperature (℃)
a	107	0.4	60-140	0.2	60	25
b	102	0.8	20-120	0.5	5	25
c	103	1.0	60-140	0.5	60	45
d	106	1.2	60-120	0.5	60	25

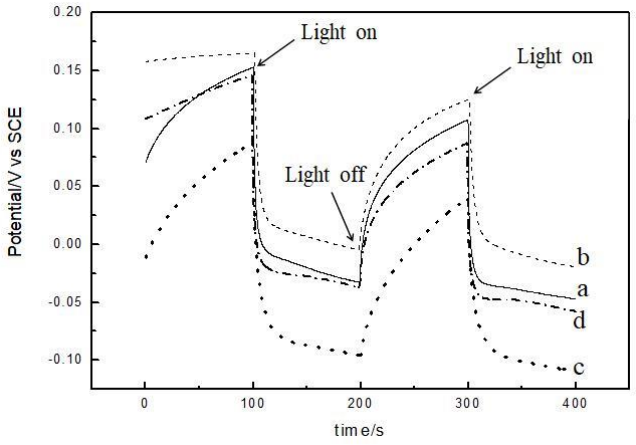

Figure 4. E_{ocp}~t curves of TiO_2 nano-porous films with ρ of 0.4×10^9 cm^{-2} (a) ρ of 0.8×10^9 cm^{-2} (b) ρ of 1.0×10^9 cm^{-2} (c) and ρ of 1.2×10^9 cm^{-2} (d).

The photoelectrochemical properties of the prepared TiO_2 nano-porous films were characterized by E_{ocp}~t curves under alternating irradiation conditions. The results are shown in figure 4. It can be detected that apparent change of the E_{ocp} occurs when the irradiation condition altered. According to the literature report, change value of E_{ocp} (expressed as ΔE) under light irradiation and non-light irradiation can be used as a standard to measure the redox ability of semiconductor electrodes and to evaluate the photoelectrochemical properties of the semiconductor materials. Large E_{ocp} variation (ΔE) expresses that the material possesses great sensitivity to light irradiation [16-18].

Based on the E_{ocp} value under light irradiation and non-light irradiation in figure 4, ΔE could be calculated and the results are listed in table 2.

Table 2. ΔE comparisons of TiO_2 nano-porous films with ρ of 0.4×10^9 cm^{-2} (a) 0.8×10^9 cm^{-2} (b) 1.0×10^9 cm^{-2} (c) and 1.2×10^9 cm^{-2} (d).

Sample	ρ ($\times10^9$ cm^{-2})	ΔE (V)
a	0.4	0.140
b	0.8	0.121
c	1.0	0.147
d	1.2	0.134

It can be found that TiO_2 nano-porous film with pore density of 1×10^9 cm^{-2} shows the highest ΔE value (equals to 0.1399 V). The ΔE value is even higher than that of heat treated titanium dioxide (under 750 ℃ in air atmosphere) reported in literature [17]. These results reveals that the TiO_2 nano-porous film with pore density of 1×10^9 cm^{-2} is the most sensitive to light and possesses the most outstanding photoelectrochemical property. However, compared with the ΔE value (above 300 mV) of the TiO_2 nanotubes obtained under the optimum heat treatment conditions reported in the literature[17-18], the ΔE values of the TiO_2 nano-porous film prepared by us still have a certain gap. In order to further improve the properties of the materials, heat treatment of the prepared TiO_2 nano-porous film can be considered in our future research.

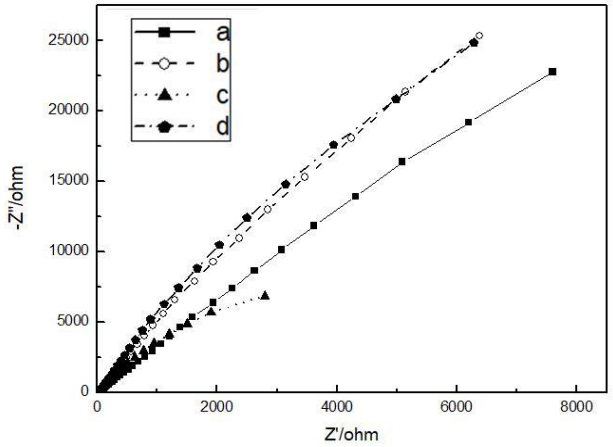

Figure 5. EIS of TiO_2 nano-porous films with ρ of 0.4×10^9 cm^{-2} (a) 0.8×10^9 cm^{-2} (b) 1.0×10^9 cm^{-2} (c) and 1.2×10^9 cm^{-2} (d) recording under the condition of non-light irradiation.

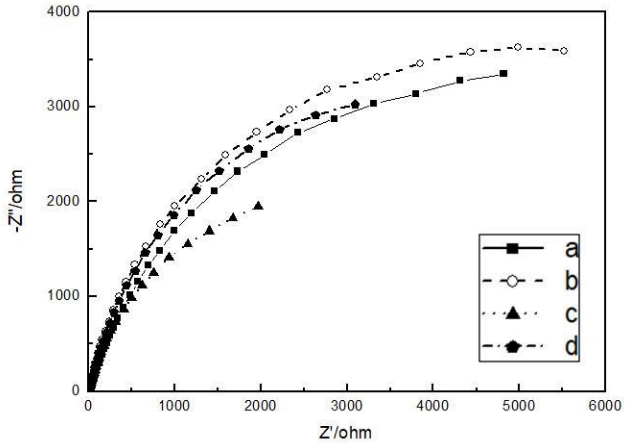

Figure 6. EIS of TiO_2 nano-porous films with ρ of 0.4×10^9 cm^{-2} (a) 0.8×10^9 cm^{-2} (b) 1.0×10^9 cm^{-2} (c) and 1.2×10^9 cm^{-2} (d) recording under the condition of light irradiation.

Electrochemical impedance spectra of the TiO_2 films with different pore density recorded under the condition of non-light irradiation and light irradiation are shown in figure 5 and figure 6. Simulated data of the electrochemical impedance spectra are listed in table 3, in which C_d represents the charging capacitor of electric double layer while R_r is the electrochemical reaction resistance. As is known to all that the lower the R_r value, the easier the electrochemical reaction. So R_r value can be used to assess the photoelectrochemical properties of TiO_2 nano-porous films. It can be seen from table 3 that the order of magnitude of R_r value obtained under the condition of non-light irradiation is in 10^{11}~10^{16} while that of R_r value obtained under the condition of light irradiation is in 10^4~10^5. Obvious reduction of the R_r value can be observed in the simulated data of all the TiO_2 films with different pore density. This reveals that all the TiO_2 films with different pore density are sensitive to the light irradiation and shows better photoelectrochemical performance under the condition of light irradiation. It can also be found that TiO_2 film with pore density of 1×10^9 cm^{-2} presents the lowest R_r value under the condition of light irradiation, which indicates that TiO_2 film with this pore density shows the optimal photoelectrochemical property. And this conclusion is in good agreement with the results obtained by E_{ocp}~t curves in table 2.

Table 3. Simulated data for EIS of TiO_2 nano-porous films with ρ of 0.4×10^9 cm^{-2} (a) 0.8×10^9 cm^{-2} (b) 1.0×10^9 cm^{-2} (c) and 1.2×10^9 cm^{-2} (d).

Sample	ρ ($\times10^9$ cm^{-2})	Non-light irradiation		Light irradiation	
		C_d(F)	R_r(Ω)	C_d(F)	R_r(Ω)
a	0.4	6.741×10^{-5}	5.563×10^{14}	1.777×10^{-4}	1.514×10^{5}
b	0.8	6.145×10^{-5}	5.356×10^{11}	1.620×10^{-4}	5.513×10^{4}
c	1.0	3.200×10^{-4}	1.027×10^{12}	4.849×10^{-4}	4.907×10^{4}
d	1.2	7.608×10^{-5}	2.232×10^{16}	1.948×10^{-4}	6.344×10^{4}

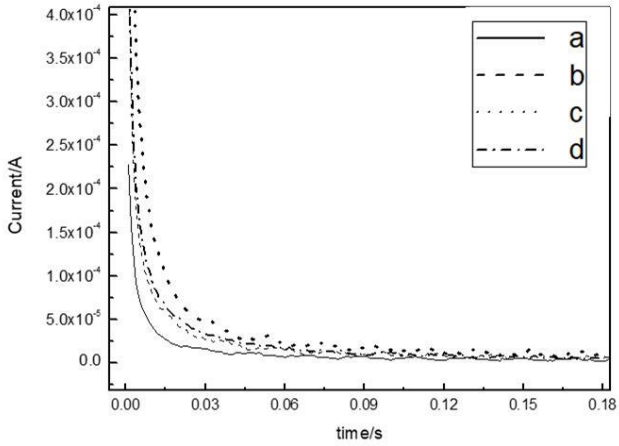

Figure 7. Chronoamperometric curves of TiO_2 nano-porous films with ρ of 0.4×10^9 cm^{-2} (a) 0.8×10^9 cm^{-2} (b) 1.0×10^9 cm^{-2} (c) and 1.2×10^9 cm^{-2} (d).

Specific surface area of the TiO_2 films with different pore density was characterized by chronoamperometry and corresponding chronoamperometric curves are shown in figure 7. Specific surface area value calculated by integal of the chronoamperometric curve are listed in table 4.

Table 4. Specific surface area of the TiO_2 nano-porous films with ρ of 0.4×10^9 cm^{-2} (a) 0.8×10^9 cm^{-2} (b) 1.0×10^9 cm^{-2} (c) and 1.2×10^9 cm^{-2} (d).

Sample	ρ ($\times10^9$ cm^{-2})	$S_{specific}$
a	0.4	27.68
b	0.8	56.88
c	1.0	111.36
d	1.2	68.18

Since enhancement of the specific surface area is beneficial for the property of the TiO_2 nano-porous films, the higher the specific surface area, the better the photoelectrochemical properties of the TiO_2 nano-porous films. It can be found from table 4 that TiO_2 film with pore density of 1×10^9 cm^{-2} presents the highest $S_{specific}$ value, which indicates that TiO_2 film with this pore density shows the optimal photoelectrochemical property.

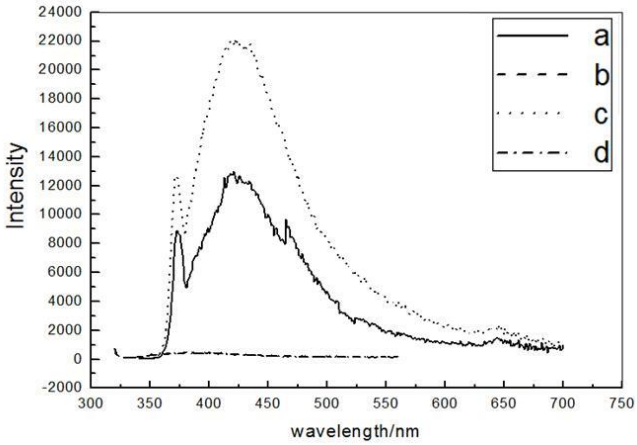

Figure 8. Fluorescence spectra of TiO_2 nano-porous films with ρ of 0.4×10^9 cm^{-2} (a) 0.8×10^9 cm^{-2} (b) 1.0×10^9 cm^{-2} (c) and 1.2×10^9 cm^{-2} (d).

To evaluate the properties of TiO_2 nano-porous films with different pore density, fluorescence spectrometry measurement was conducted in the wavelength range of 300~700 nm (Figure 8). Peak intensity and peak location of the fluorescence spectra in figure 8 are listed in Table 5. Since intensity of the emission peak in fluorescence spectra can be used to appraise the photochemical properties of the TiO_2 nano-porous films [16], high emission peak intensity implies great photochemical properties. Comparing the curves and data in figure 7 and table 5, it can be found that TiO_2 nano-porous film with pore density of 1×10^9 cm^{-2} exhibits the highest peak intensity (equals to 14428), which means that the TiO_2 nano-porous film with this pore density has the optimal photochemical property.

Table 5. Peak intensity and location of the fluorescence spectra in figure 8

Sample	ρ ($\times10^9$ cm^{-2})	Peak intensity	Peak location (nm)
a	0.4	12896	422
b	0.8	482	425
c	1.0	14428	426
d	1.2	463	423

Table 6. Peak intensity and location of the ultraviolet spectra in figure 9

Sample	ρ ($\times10^9$ cm^{-2})	Peak intensity	Peak location (nm)
a	0.4	0.66	354
b	0.8	0.70	355
c	1.0	0.72	369
d	1.2	0.67	354

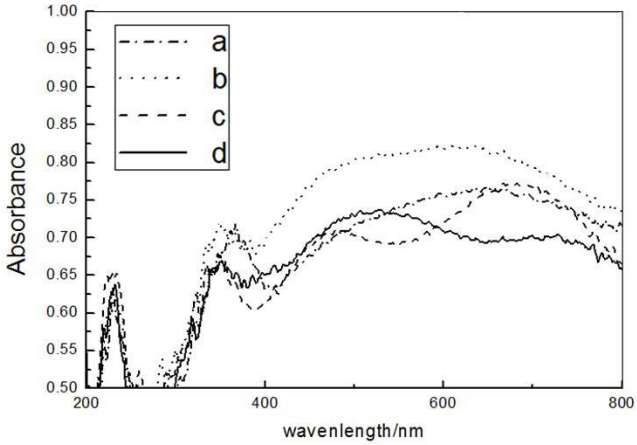

Figure 9. UV-vis absorption spectra of TiO_2 nano-porous films with ρ of 0.4×10^9 cm^{-2} (a) 0.8×10^9 cm^{-2} (b) 1.0×10^9 cm^{-2} (c) and 1.2×10^9 cm^{-2} (d).

TiO_2 nano-porous films with different pore density were also characterized by UV-vis absorption spectrometry. The results are demonstrated in figure 9 and table 6. It can be seen that the maximum absorption peak of all the TiO_2 nano-porous films with different pore density located in ultraviolet spectrum region, which means that the TiO_2 nano-porous films have strong absorption to ultraviolet light. It can also be found from table 6 that TiO_2 nano-porous film with pore density of 1×10^9 cm^{-2} shows the highest absorption peak intensity value (equals to 0.72), which reveals that the TiO_2 nano-porous film with this pore density is the most sensitive to UV light and possesses the best photoelectrochemical property.

Based on the above analysis, we can conclude that the optimum pore density of TiO_2 nano-porous films is 1×10^9 cm^{-2}.

3.2 Effects of average aperture on the photoelectrochemical properties of TiO_2 nano-porous thin films

In order to investigate the effects of average aperture on the photoelectrochemical performance of TiO_2 nano-porous thin films, a group of samples with different average aperture but pore density of about 1.0×10^9 cm^{-2} (based on the discuss in 3.1) were prepared according to our earlier research [15, 19]. The details of the preparation parameters and the average aperture and pore density of the samples are listed in Table 7.

Table 7. Preparation parameters of TiO_2 nano-porous films with $\bar{d}$ of 95 nm (a) 103 nm (b) 112 nm (c) and 130 nm (d).

Sample	$\bar{d}$ (nm)	ρ ($\times10^9$ cm^{-2})	Initial voltage-discharge voltage (V)	Electrolyte concentration ($mol\cdot l^{-1}$)	Time (min)	Temperature (℃)
a	95	0.8	60-120	0.5	5	25
b	103	1.0	60-140	0.5	60	45
c	112	1.0	60-140	0.5	30	25
d	130	0.9	80-120	0.5	5	25

Table 8. ΔE comparisons of TiO_2 nano-porous films with $\bar{d}$ of 95 nm (a) 103 nm (b) 112 nm (c) and 130 nm (d).

Sample	$\bar{d}$ (nm)	ΔE (V)
a	95	0.093
b	103	0.147
c	112	0.126
d	130	0.112

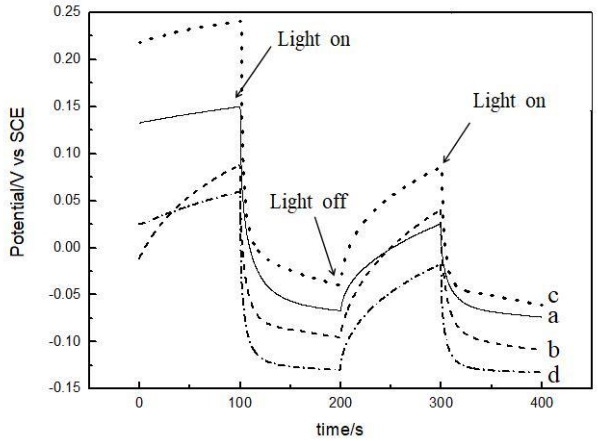

Figure 10. E_{ocp}~t curves of TiO_2 nano-porous films with $\bar{d}$ of 95 nm (a) 103 nm (b) 112 nm (c) and 130 nm (d).

The photoelectrochemical properties of the prepared TiO_2 nano-porous films were characterized by the E_{ocp}~t curves under the condition of light irradiation and non-light irradiation. The results are demonstrated in figure 10 and the ΔE values are listed in table 8. It can be seen from table 8 that TiO_2 nano-porous film with $\bar{d}$ of 103 nm shows the highest ΔE value, which reveals that the TiO_2 nano-porous film with average aperture of 103 nm is the most sensitive to light and possesses the best photoelectrochemical property.

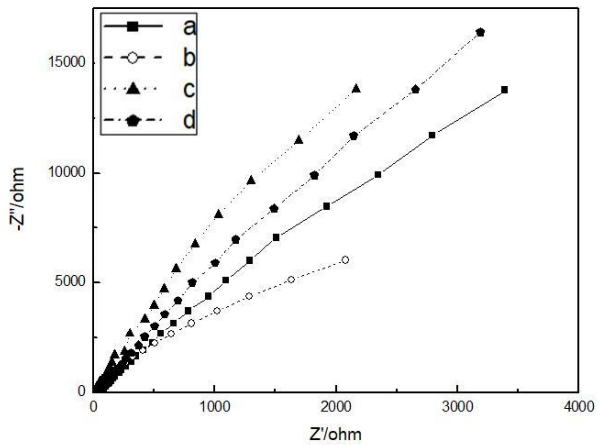

Figure 11. EIS of TiO_2 nano-porous films with $\bar{d}$ of 95 nm (a) 103 nm (b) 112 nm (c) and 130 nm (d) recording under the condition of non-light irradiation.

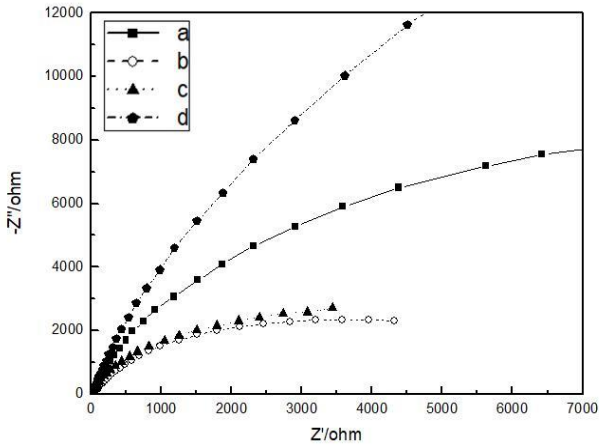

Figure 12. EIS of TiO_2 nano-porous films with $\bar{d}$ of 95 nm (a) 103 nm (b) 112 nm (c) and 130 nm (d) recording under the condition of light irradiation.

EIS of the TiO_2 films with different average aperture recorded under the condition of non-light irradiation and light irradiation are shown in figure 11 and figure 12. Simulated data of the electrochemical impedance spectra are listed in table 9. It can be found from table 9 that the order of magnitude of R_r value obtained under the condition of non-light irradiation is in 10^{12}~10^{16} while that of R_r value obtained under the condition of light irradiation is in 10^4~10^5. Obvious reduction of the R_r value can be observed in the simulated data of EIS for all the TiO_2 films with different average aperture. This reveals that all the TiO_2 films with different average aperture are sensitive to sunlight. It can also be found that TiO_2 film with average aperture of 103 nm shows the lowest R_r value under the condition of light irradiation, which indicates that TiO_2 film with this average aperture possesses the best photoelectrochemical property. And this conclusion matches well with that obtained by E_{ocp}~t curves in table 8.

Table 9. Simulated data for EIS of TiO_2 nano-porous films with $\bar{d}$ of 95 nm (a) 103 nm (b) 112 nm (c) and 130 nm (d).

Sample	$\bar{d}$ (nm)	Non-light irradiation		Light irradiation	
		C_d(F)	R_r(Ω)	C_d(F)	R_r(Ω)
a	95	5.387×10^{-5}	1.026×10^{14}	4.548×10^{-4}	1.155×10^{5}
b	103	3.200×10^{-4}	1.027×10^{12}	7.213×10^{-4}	1.069×10^{4}
c	112	5.267×10^{-4}	3.858×10^{15}	1.931×10^{-4}	1.983×10^{4}
d	130	2.616×10^{-4}	2.232×10^{16}	5.379×10^{-4}	3.275×10^{4}

Specific surface area of the TiO_2 films with different average aperture was characterized by chronoamperometry and corresponding chronoamperometric curves are shown in figure 13. Specific surface area value calculated by integal of the chronoamperometric curve are listed in table 10. It can be seen from table 10 that TiO_2 film with the average aperture of 103 nm shows the highest $S_{specific}$

value, which indicates that TiO_2 film with this average aperture owns the best photoelectrochemical property.

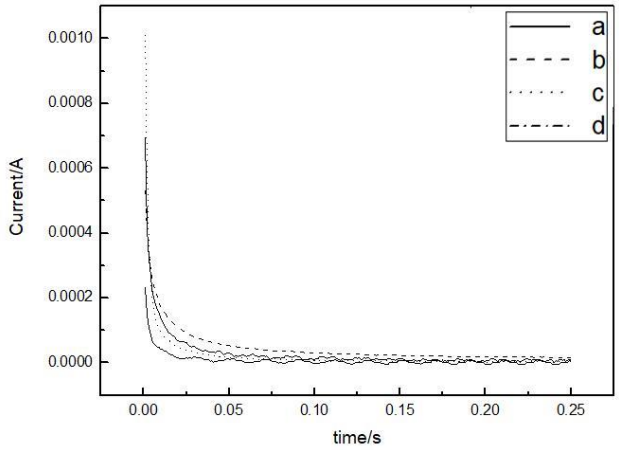

Figure 13. Chronoamperometric curves of TiO_2 nano-porous films with $\bar{d}$ of 95 nm (a) 103 nm (b) 112 nm (c) and 130 nm (d).

Table 10. Specific surface area of the TiO_2 nano-porous films with $\bar{d}$ of 95 nm (a) 103 nm (b) 112 nm (c) and 130 nm (d).

Sample	$\bar{d}$ (nm)	$S_{specific}$
a	95	24.18
b	103	138.40
c	112	95.98
d	130	63.52

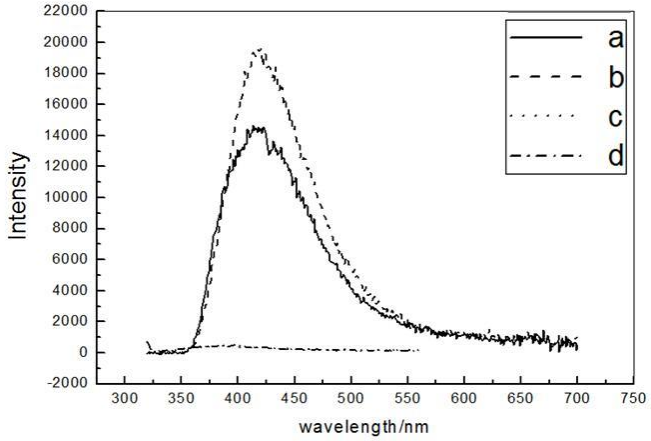

Figure 14. Fluorescence spectra of TiO_2 nano-porous films with $\bar{d}$ of 95 nm (a) 103 nm (b) 112 nm (c) and 130 nm (d).

To evaluate the properties of TiO_2 nano-porous films with different average aperture, fluorescence spectrometry measurement was conducted in the wavelength range of 300~700 nm (Figure 14). Peak intensity and peak location of the fluorescence spectra in figure 14 are listed in Table 11. It can be seen that TiO_2 nano-porous film with average aperture of 103 nm exhibits the highest

peak intensity value (equals to 19409), which indicates that the TiO_2 nano-porous film with this average aperture is the most sensitive to light and has the best photoelectrochemical property.

Table 11. Peak intensity and location of the fluorescence spectra in figure 14

Sample	$\bar{d}$ (nm)	Peak intensity	Peak location (nm)
a	95	14290	413
b	103	19409	419
c	112	193	400
d	130	409	415

Table 12. Peak intensity and location of the ultraviolet spectra in figure 15

Sample	$\bar{d}$ (nm)	Peak intensity	Peak location (nm)
a	95	0.66	358
b	103	0.72	369
c	112	0.71	366
d	130	0.69	349

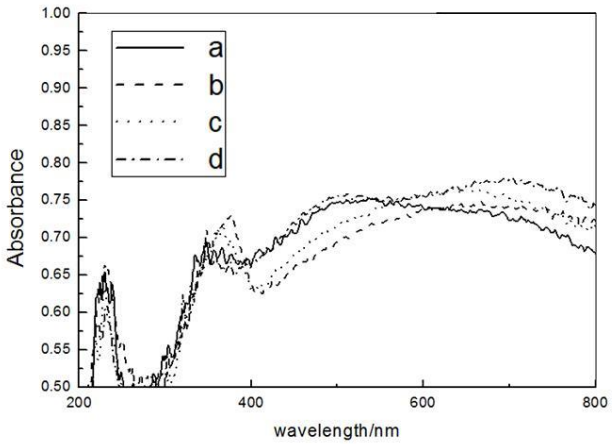

Figure 15. UV-vis absorption spectra of TiO_2 nano-porous films with $\bar{d}$ of 95 nm (a) 103 nm (b) 112 nm (c) and 130 nm (d).

TiO_2 nano-porous films with different average aperture were also tested by UV-vis absorption spectrometry. And the results are demonstrated in figure 15 and table 12. It can be found from figure 15 and table 12 that TiO_2 nano-porous film with average aperture of 103 nm exhibits the highest absorption peak intensity value (equals to 0.72), which illustrates that the TiO_2 nano-porous film with this average aperture is the most sensitive to UV light and owns the best photoelectrochemical property. This conclusion matched well with that obtained by E_{ocp}~t curves, EIS, chronoamperometry and fluorescence spectrometry.

Based on the above analysis, we can see that the optimum average aperture of TiO_2 nano-porous films is 103 nm.

4. CONCLUSIONS

In this paper, TiO_2 nano-porous thin films with different average aperture and pore density were fabricated by electrochemical anodic oxidation. Effects of average aperture and pore density on the photoelectrochemical properties and the specific surface area of the TiO_2 nano-porous thin films were investigated by various electrochemical and spectrum measurement, including E_{ocp}~t curves, EIS, chronoamperometry, fluorescence spectrometry and UV-vis absorption spectrometry. The results indicated that all the TiO_2 films with different pore density and average aperture were sensitive to the light irradiation and showed better photoelectrochemical performance under the condition of light irradiation. The larger the specific surface area, the better the photoelectrochemical performance. TiO_2 nano-porous thin film with the average aperture and pore density of 103 nm and 1×10^9 cm^{-2}, respectively, possessed the best photoelectrochemical property.

ACKNOWLEDGEMENTS
The authors gratefully acknowledge the financial support from the Tianjin Municipal Education Committee Project (160020), National Science Foundation of China (51802222) and Tianjin University Innovation Team Project (TD135087).

References

1. M.B. Sarkar, B. Choudhuri, P. Bhattacharya, R.N. Barman, A. Ghosh, S.M.M.D Dwivedi, S. Chakrabartty and A. Mondal, *J. Nanosci. Nanotechno.,* 18 (2018) 4898.
2. T. Dikici and M. Toparli, *Mat. Sci. Eng. A,* 661 (2016) 19.
3. L. Predoana, I. Stanciu, M. Anastasescu, J.M. Calderon-Moreno, M. Stoica, S. Preda, M. Gartner, M. Zaharescu, *J. Sol-Gel. Sci. Technol.,* 78 (2016) 589.
4. Q.F. Song, Y.J. Zhu, H.K. Zheng, F.B. Zhang and M.X. Wu, *Mater. Design,* 98 (2016) 108.
5. Z. Wang and X.J. Lang, *Appl. Catal. B-Environ.,* 224 (2018) 404.
6. A.W. Wren, B.M. Adams, D. Pradhan, M.R. Towler and N.P. Mellott, *Mater. Chem. Phys.,* 144 (2014) 538.
7. J.K. Chen, W.Y. Fu, G.Y. Yuan, A. Runa, H. Bala, X.D. Wang, G. Sun, J.L. Cao and Z.Y. Zhang, *Mater. Lett.,* 135 (2014) 229.
8. Z.Y. Zhao, Y. Zhou, W.C. Wan, F. Wang, Q. Zhang and Y.H. Lin, *Mater. Lett.,* 130 (2014) 150.
9. S. Palmas, A.D. Pozzo, M. Mascia, A. Vacca, A. Ardu, R. Matarrese and I. Nova, *Int. J. Hydrogen. Energy,* 36 (2011) 8894.
10. G.X. Zhang, X.B. Dong and S.L. Zheng, *J. Inorg. Mater.,* 31 (2016) 407.
11. J. Zhang, B. Wu, L.H. Huang, P.L. Liu, X.Y. Wang, Z.D. Lu, G.L. Xu, E.P. Zhang, H.B. Wang, Z. Kong, J.H. Xi and Z.G. Ji, *J. Alloy. Compd.,* 661 (2016) 441.
12. H.H. Yan, T.J. Zhao, X.J. Li and C.H. Hun, *Ceram. Int.,* 41 (2015) 14204.
13. H.L. Liang, Y.X. Wu, J. Tang, Y.L. Huo, H.L. Liu and Y.F. Chen, *Rare. Metal. Mat. Eng.,* 44 (2015) 605.
14. Y. Wang, Y.M. He, Q.H. Lai and M.H. Fan, *J. Environ. Sci-China,* 26 (2014) 2139.

15. Y.L. Gong, Y.X. Ren, Y. Yang, Z.C. Bai and H.T. Guo, *J. Chem. Ind. Eng-China,* 58 (2007) 3185.
16. Y.L. Gong, F.H. Li, F. Lu and C. Dai, *Bull. Mater. Sci*., 38 (2015) 847.
17. C. Jin, W.G. Zhang, S.W. Yao, H.Z. Wang, *J. Inorg. Mater.,* 27 (2012) 54.
18. H.Y. Li, J.S. Wang, J. Ran, M.L. Zhou, *Chin. J. Nonferrous. Met.*, 19 (2009) 1119.
19. Y.L. Gong, F.H. Li, Z.C. Bai and Y. Yang, *Plat. Finish-China,* 32 (2010) 5.